Received: 10 July 2024 | Revised: 8 January 2025 | Accepted: 18 February 2025

DOI: 10.1002/suco.202400902

ARTICLE

fib CEB-FIP WILEY

Long-term mechanical properties of hybrid fiber-reinforced engineered cementitious composite

Shiyao Zhu[1,2] | **Y. X. Zhang**[2] | **C. K. Lee**[1]

[1]School of Engineering and Technology, University of New South Wales, Canberra, Australian Capital Territory, Australia

[2]School of Engineering, Design and Built Environment, Western Sydney University, Kingswood, New South Wales, Australia

Correspondence
C. K. Lee, School of Engineering and Technology, University of New South Wales, Canberra, Australian Capital Territory 2600, Australia.
Email: chi.k.lee@unsw.edu.au

Abstract

Hybrid fiber-reinforced engineered cementitious composites (hybrid ECC) employing short straight polyethylene (PE) and steel fibers have attracted growing interest in engineering applications due to their superior strength and ductility. In most studies, the mechanical properties of hybrid ECC were determined based on samples cured for 28 days, while their long-term mechanical properties are seldom studied. Since hybrid ECCs often incorporate supplementary cementitious materials that alter the hydration process over time, relying solely on the 28-day strength of samples may lead to inaccurate structural designs. To better understand the long-term mechanical properties of hybrid ECC, this work presents an experimental investigation of hybrid PE-steel fiber-reinforced ECC samples cured under standard conditions for up to *3 years*. Uniaxial compressive tests, direct tensile tests, and four-point bending tests were conducted with samples cured at standard conditions for *28 days*, *1 year*, and *3 years*. It was found that the compressive and tensile strengths of hybrid ECC increased with age. However, as the age increased to 3 years, the ultimate tensile strain and flexural ductility decreased significantly by 54% and 35%, respectively, compared to their 28-day values. Furthermore, most changes occurred within 1 year. It was also found that the main damage pattern of the PE fibers was transformed from pull-out to rupture failure as the curing age increased. Thermal-gravity analysis revealed that the hydration process of hybrid ECC may last for up to 3 years, which explains their changes in mechanical properties and PE fiber failure mode.

KEYWORDS

ductility, engineered cementitious composite (ECC), hybrid fibers, long-term behavior, mechanical properties

1 | INTRODUCTION

Engineered cementitious composites (ECC) are manufactured by using cement, aggregates, supplementary cementitious material (SCM), fibers, and water. Similar to normal concrete, fresh ECC hardens as age increases and then gains strength gradually. In most studies, the typical way to determine the mechanical properties of hybrid ECC is to test samples cured at standard conditions for 28 days.[1–3] However, it was reported that some mechanical properties

of ECCs, such as the ultimate tensile strain, could decrease after a certain period.[4–6] Much research reported that well-formulated ECCs demonstrated high ductility at the age of 28 days. Li et al. developed a mix design of polyvinyl alcohol (PVA) fiber-reinforced ECC,[7] which showed a high ductility of 4.5% (direct tensile strain) when tested after 28 days under standard curing conditions. Yu et al.[8] developed a polyethylene (PE) fiber-reinforced ECC with a high tensile strain of up to 8% at 28 days.

ECCs commonly incorporate SCMs such as fly ash and silica fume.[4,9–13] It has been found that the pozzolanic reaction of fly ash was slow at early ages and more than 80% of the fly ash could remain unreacted even after 90 days of curing.[14,15] The use of a high-volume fraction of fly ash in ECCs could lead to a long hydration process. Therefore, the interface between fibers and the matrix may experience significant changes after long-term curing that eventually affect the long-term mechanical behavior of ECC. The study done by Lepech and Li[4] reported that the ultimate tensile strain of their PVA-ECC decreased from 5% at 28 days to 3% at 180 days. Another study by Lu et al.[9] also found that the ultimate tensile strain of their PVA-ECC was 1.31% at 180 days and reduced to 0.97% at 1 year, which was significantly less than that of 6.13% tested at 28 days. Considering the reduction of ultimate tensile strain observed over time and the much longer design life in all structural applications, the use of mechanical properties (especially ductility) at 28 days as design parameters could be inappropriate.

Few studies have been carried out on investigating the long-term mechanical properties of ECCs, especially for specimens cured longer than 1 year. To better understand hybrid ECC's long-term behavior, it is essential to conduct an experimental investigation on the change of mechanical properties over time. One of the challenges for conducting such a study is the long curing time required, especially when standard curing is used to replicate the natural curing conditions in actual applications, as changes in the mechanical properties and ductility may last for up to 1 year or even longer.[4,5] Lepech and Li[4] tested the tensile strain capacity of their ECC at the age of 180 days and compared it to that tested at early age with an observation of around a 40% decrease. Due to the limitation of their test program, it was uncertain about the changing trend beyond 180 days. Accelerated tests were conducted by Li et al.[5] who studied the tensile strength and strain of PVA-ECC at different curing days. Samples were cured in a water tank at 20°C for 28 days and then followed by accelerated curing, where they were immersed in water at 60°C for 4, 13, and 26 weeks, respectively. It was observed that the ultimate tensile strain decreased from 4.47% at 28 days to 2.72% at 28 days + 26 weeks. Such a decrease in long-term ductility might be caused by the interaction between fibers and the matrix over time. However, the exact mechanism behind such changes was not reported, and changes after 28 days + 26 weeks were not studied in Li et al.[5] In addition, even fewer attentions were paid to the long-term changes in compressive and flexural properties. For construction materials used for structural applications, long-term changes in tensile, compressive, and flexural properties are critical for evaluating their structural performance.

This work presents an experimental study on the long-term mechanical properties of hybrid ECC for up to 3 years. The hybrid ECC studied in this work employing PE and steel fibers was developed by the authors for bridge link slab applications.[16] The long-term compressive, tensile, and flexural properties of this hybrid PE-Steel ECC were studied by curing the samples under standard curing conditions to replicate actual maturing conditions in practical applications. Microscopic analysis and thermogravimetric analysis (TGA) were also conducted to gain a better understanding of the hydration behaviors and fiber–matrix interaction as age increases.

2 | RESEARCH SIGNIFICANCE

This study addresses the gap in the long-term mechanical characterization of ECC that currently attract much interest in the structural applications of ECCs due to their high strength and ductility. While most studies evaluate the mechanical properties of ECCs at 28 days, evidence shows that many critical properties, such as ultimate tensile strain, can degrade over time, potentially impacting long-term structural performance. This research presents a comprehensive experimental investigation studying the long-term mechanical properties of a novel hybrid ECC developed with PE and steel fibers. The research findings highlight the importance of understanding the long-term maturity of ECC when formulating ECC mix designs optimized for structural longevity.

3 | EXPERIMENTAL PROGRAMME

3.1 | Hybrid ECC mix preparation

A carefully developed mix design of hybrid ECC employing PE and steel fibers[16] for bridge link slab applications was adopted in this study. The mix proportions are shown in Table 1. In this mix design, SCM including silica fume and fly ash was used. Local (Bungendore) sand was used with a maximum particle size of 300 μm. In addition, a high-range water reducer (HRWD) was used to maintain the workability and quality of the fresh mix. Hybrid fibers of 1.25% PE fiber and 0.75% steel fiber in

TABLE 1 Mix proportions of polyethylene (PE)-steel ECC.

Cement	Silica fume	Fly ash	Local sand	Water	HRWR	PE	ST
Ratio to binder (wt%)						Volume fraction (vol%)	
0.58	0.1	0.32	0.4	0.24	0.008	1.25	0.75

Abbreviations: binder, cement + silica fume + fly ash; HRWR, high-range water reducer (superplasticizer); ST, steel fiber.

TABLE 2 Material properties of polyethylene (PE) fiber and steel fiber.

Fibers	Diameter (μm)	Length (mm)	Ultimate tensile strength (MPa)	Young's modulus (GPa)
PE	23	12	3000	110
Steel	200	13	3200	200

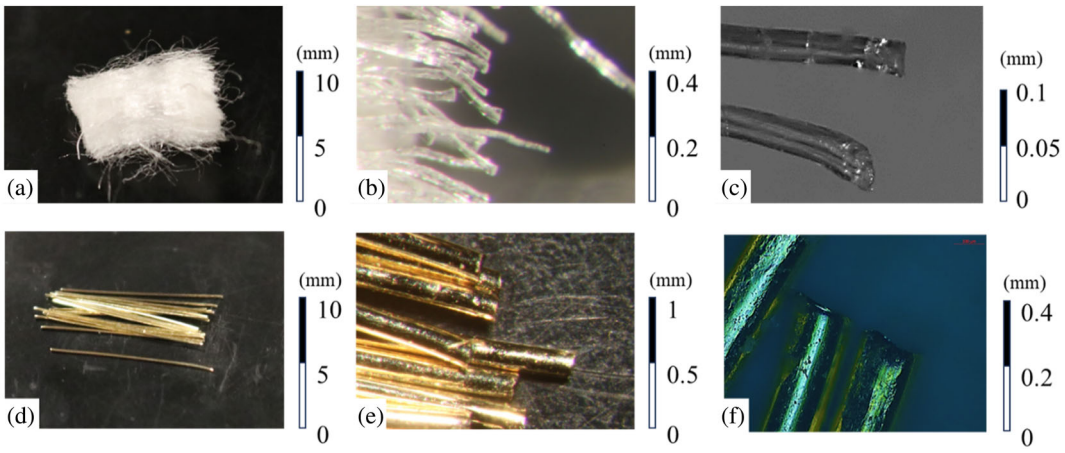

FIGURE 1 Profiles of polyethylene fibers (a–c) and steel fibers (d–f) at different magnifications.

volume fraction were used. The material properties of the fibers are shown in Table 2. Images of pristine PE and steel fibers taken under an optical microscope at different scales are shown in Figure 1.

3.2 | Samples preparation and test schemes

Samples cured for 28 days (28d), 1 year (1y), and 3 years (3y) were used to investigate the long-term mechanical properties of the hybrid ECC. In order to replicate maturing conditions in practical applications, all samples were cured under standard conditions in a fog room where the temperature was kept at 23 ± 2°C while the relative humidity was kept at 95% ± 5%. All samples were prepared with the same mix design and raw materials for consistency. Mechanical properties, including compressive properties, tensile properties, and flexural properties, were studied using standard tests. For each curing duration (28d, 1y, and 3y), six cylinders of 100 mm diameter and 200 mm height were prepared. Among the six cylinders prepared for each curing duration, three of them were used for uniaxial compression tests to obtain the compressive strength, while another three were used for retrieving the Young's modulus. Uniaxial compression tests were conducted according to ASTM C39.[17] The test was conducted at a rate of 0.05 mm/min with deformation control, with three linear variable differential transformers (LVDTs) attached to the cylinders to record the strain development until the samples failed. Young's modulus was determined in accordance with ASTM C469[18] based on the same test set-up, with a loading rate of 0.33 MPa/s applied for three full repeated cycles of loading and unloading.

Dog-bone samples (Figure 2) were employed for direct tensile tests using a set-up described in.[16,19] Digital image correlation (DIC) was applied for strain analysis and evaluated the cracking behavior of the samples. Aging effects on tensile strength, ultimate tensile strain, and cracking behavior were investigated by testing samples with different curing ages. For each curing age, six dog-bone samples were tested.

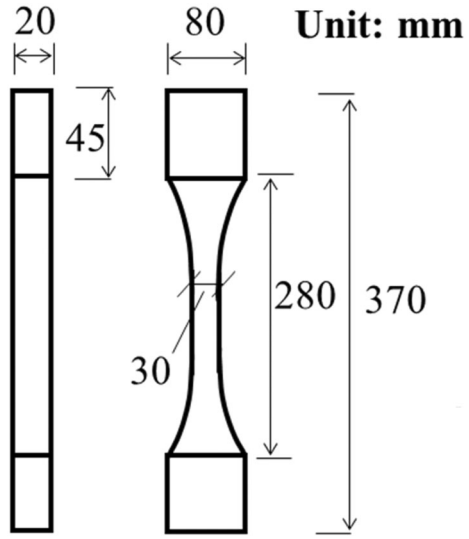

FIGURE 2 Dog-bone sample for direct tensile tests.

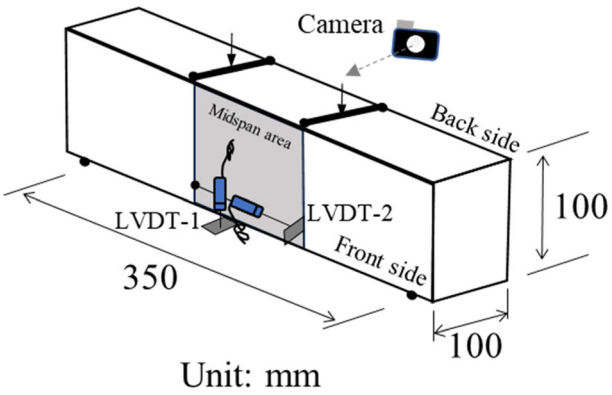

FIGURE 3 Small beam sample for four-point bending test. LVDT, linear variable differential transformers.

Small beams with a length of 350 mm, a width of 100 mm, and a height of 100 mm were used for flexural tests (Figure 3). The flexural behavior of the beams was investigated by a standard four-point bending test according to ASTM C1609.[20] The test was conducted at a loading rate of 0.05 mm/min with deformation control. During the loading process, two LVDTs were employed to record the midspan deflection (LVDT-1) and the total crack mouth opening displacement (TCMOD; LVDT-2). A high-resolution digital camera was used to take images for tracking the crack development. The flexural strength, ductility, and cracking behavior were analyzed. For the flexural test, three specimens each were tested for 28d and 3y samples only.

TGA was performed using a simultaneous thermal analyzer, NETZSCH STA 449 F3 Jupiter. Tested samples were pretreated with isopropanol to arrest the hydration process at the tested date. The tested samples were then dried and pulverized into a fine powder. For each test, 10 mg of crushed sample was heated up to 1100°C at a rate of 5°C/min under a flow of nitrogen at a rate of 20 mL/min. Weight loss measured by TGA at different ages was analyzed.

ZEISS Axioscope light microscope and HITACHI TM3000 scanning electron microscope (SEM) were utilized to observe the microstructure of samples at different ages. Tested samples were prepared and cut out from the fractured dog-bone samples after the direct tensile test. Magnification levels ranging from 12 to 1000 times were selected for observations of damage patterns of PE fibers and steel fibers at different scales.

4 | TEST RESULTS AND DISCUSSIONS

4.1 | Microscopic observations

Distinct damage patterns of fibers were observed at different curing ages via an optical microscope to obtain a broad vision at a relatively low level of magnitude (×12 to ×24). As shown in Figure 4a, at the fracture region of 28d dog-bone samples, more PE fibers showed smooth surfaces (yellow rectangles) and fibrillation ends (yellow circles) than those of 1y and 3y samples. This indicates that at an early curing age, more PE fibers were pulled out from the ECC matrix rather than ruptured. The pull-out behavior of fibers relies on the condition that the fiber tensile strength is greater than the friction between the fiber and matrix (i.e., average bond strength with the matrix). As shown in Figure 4b,c, at 1y and 3y, more PE fibers showed rough surfaces and blunt ends, which are distinct from images at an early age (Figure 4a). This indicates that more fibers were ruptured rather than being pulled out from the matrix. Such a change of damage mode could be caused by the increasing friction (i.e., average bond strength) between the fiber and matrix due to continuous hydration as age increases. As a result, the fiber strength was lower than the average bond strength between the fiber and matrix and eventually led to more fibers ruptured at later ages.

More detailed observations on fiber surfaces and ends with higher magnifications (×50 to ×100) are shown in Figure 5. Figure 5a clearly shows that PE fibers at 28d have smooth surfaces (yellow rectangle) and fibrillation ends (yellow circle). The smooth surface is similar to the original fiber surfaces as shown in Figure 1c, while the ends are different. The fibrillation end is formed by scratching when PE fibers are pulled out from the matrix. Compared with 28d samples, damage patterns of PE fiber from 1y and 3y samples were different. Figure 6 shows

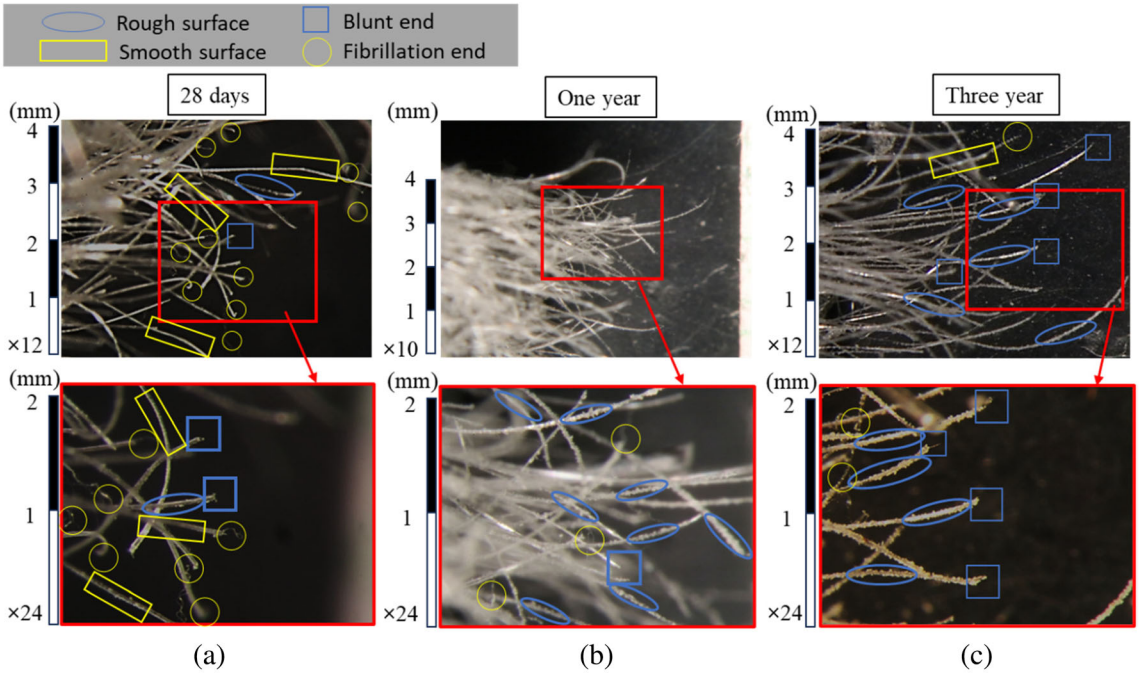

FIGURE 4 Damaged polyethylene fibers surface and ends observed at (a) 28 days, (b) 1 year, and (c) 3 years after direct tensile tests.

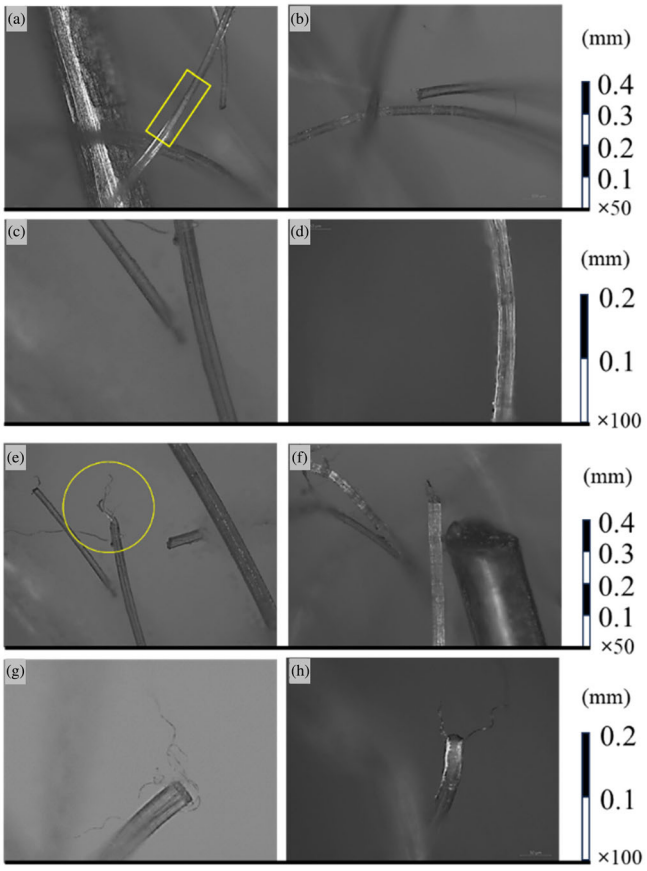

FIGURE 5 Observation of damaged polyethylene fibers surfaces (a–d) and ends (e and f) at 28 days.

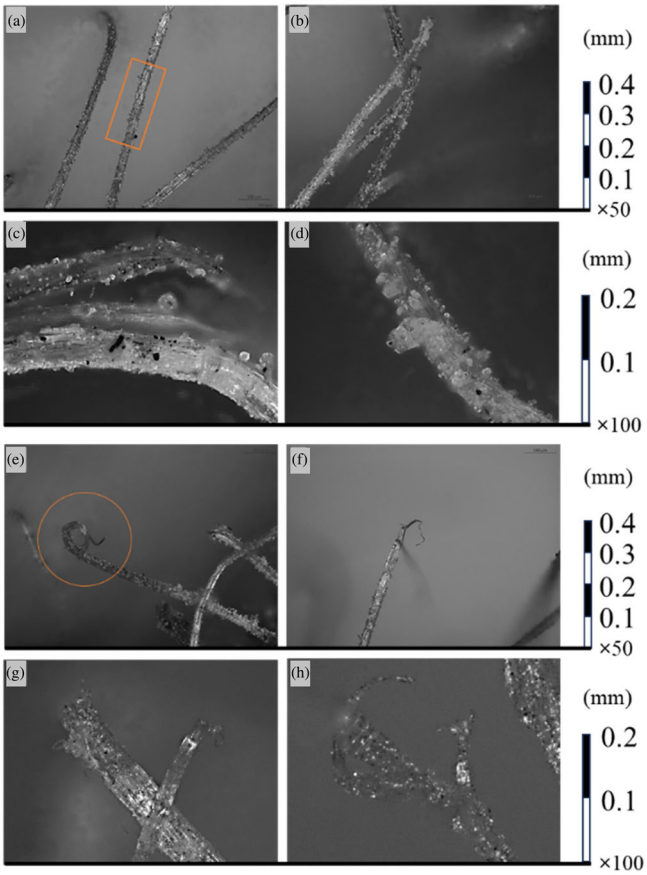

FIGURE 6 Observation of damaged polyethylene fibers surfaces (a–d) and ends (e and f) at 3 years.

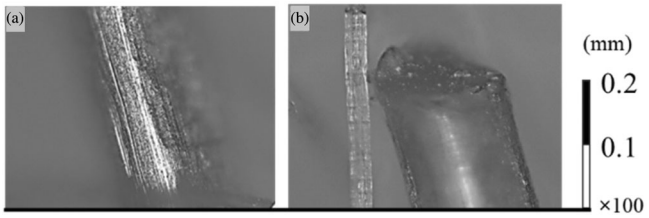

FIGURE 7 Observation of (a) steel fiber surfaces and (b) ends at 28 days.

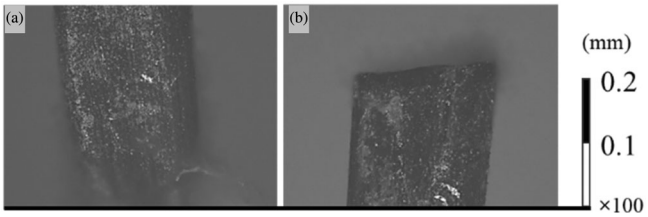

FIGURE 8 Observation of (a) steel fiber surfaces and (b) ends at 3 years.

the microscopic observations of 3y samples (appearance of 1y samples is very similar to 3y samples so is not presented here). Figure 6a–d show that some fine particles were attached to the PE fiber surfaces (orange rectangle). Blunt ends of fibers shown in Figure 6e–h showed that the fibers were severely damaged. Splitting and curling were observed where the fiber ends were frayed or separated into smaller strands. Furthermore, some fibers were twisted/bent into a curly shape due to the snap-back effect after fibers rupture.

Figures 7 and 8 show images of steel fibers at the fracture area after 28d and 3y curing, respectively. It is observed that steel fibers are pulled out from the matrix regardless of age. This is due to their much higher tensile strength (diameter of steel fiber is more than eight times of PE fiber, Table 1), which is stronger than the average bond strength. As shown in Figures 7 and 8, no visual difference was observed on the steel fiber surface nor at the fiber ends at different ages when compared to the original steel fibers (Figure 1e,f). Hence, it can be concluded that the long-term behaviors of hybrid ECCs were not seriously affected by the behaviors of steel fibers.

From the microscopic observations and analyses, it is found that while PE fibers demonstrate pull-out behavior at 28d, their main failure mode was changed to rupture failure for specimens cured 1y and 3y. It is expected that such a failure mode change might cause changes in mechanical properties and ductility.

Observations under SEM illustrate more details of PE fiber damage and the interface between fibers and matrix. At 28d, as shown in Figure 9a,b, smooth surfaces with scratching and fibrillation ends were clearly observed, which again confirms the pull-out failure mode for PE fibers. Figure 9c shows a trail left behind after the fiber was pulled out. It is interesting to note that some unhydrated fly ash round particles were observed for 28d sample (Figure 9d). For 3y samples, some hydration products attached to PE fiber were observed, as shown in Figure 10a,b, which explains the increasing friction/bond strength between fiber and matrix and the rupture of PE fibers. The splitting fiber end shown in Figure 10c further confirms the rupture of PE fibers. In particular, further hydration of fly ash was observed, with hydration products gradually covering the round fly ash particles at the highlighted area in Figure 10d. This confirms that continuous hydration could develop until 3 years. It should also be mentioned that from the SEM analysis, no substantial differences were observed in samples tested at 1 and 3 years.

4.2 | Thermogravimetric (TG) analysis

The hydration reaction in ECC primarily involves the interaction of water with cementitious materials, including cement, fly ash, and silica fume, resulting in the formation of calcium silicate hydrate and portlandite.[21] It is known that the decomposition of cement hydrates is generally divided into three main phases, namely, (i) decomposition of hydrates, (ii) dehydroxylation of portlandite, and (iii) decarbonation of calcite.[22,23] The first phase, which occurs between 25 and 400°C, consists of mass loss related to the evaporation of water and decomposition of hydrates. The loss of free water occurs between 25 and 105°C, while the decomposition of hydrates occurs between 105 and 400°C. The second phase of dehydroxylation of portlandite normally occurs between 400 and 600°C. The third phase of decarbonation of calcite normally occurs between 600 and 800°C.

Figure 11 shows the mass loss (TG) curves and the first derivation of the TG (DTG) curves of hybrid ECC samples at 28d, 1y, and 3y of curing. Three significant drops (indicated with the black dot) were observed on the DTG curves regardless of the ages, which represent the decomposition of hydrates, the dehydroxylation of portlandite, and the decarbonation of calcite, respectively. The mass loss curves 28d (black solid line), 1y (orange solid line), and 3y (green solid line) are analyzed and compared. The accumulated mass losses at different temperature ranges (i.e., 25–400, 400–600, and 600–800°C) are calculated and given in Table 3. It is found that at 28d, the mass loss between 25 and 400°C is 9.13%, which is higher than the values observed for 1y and 3y samples. This indicates that more free and bound water

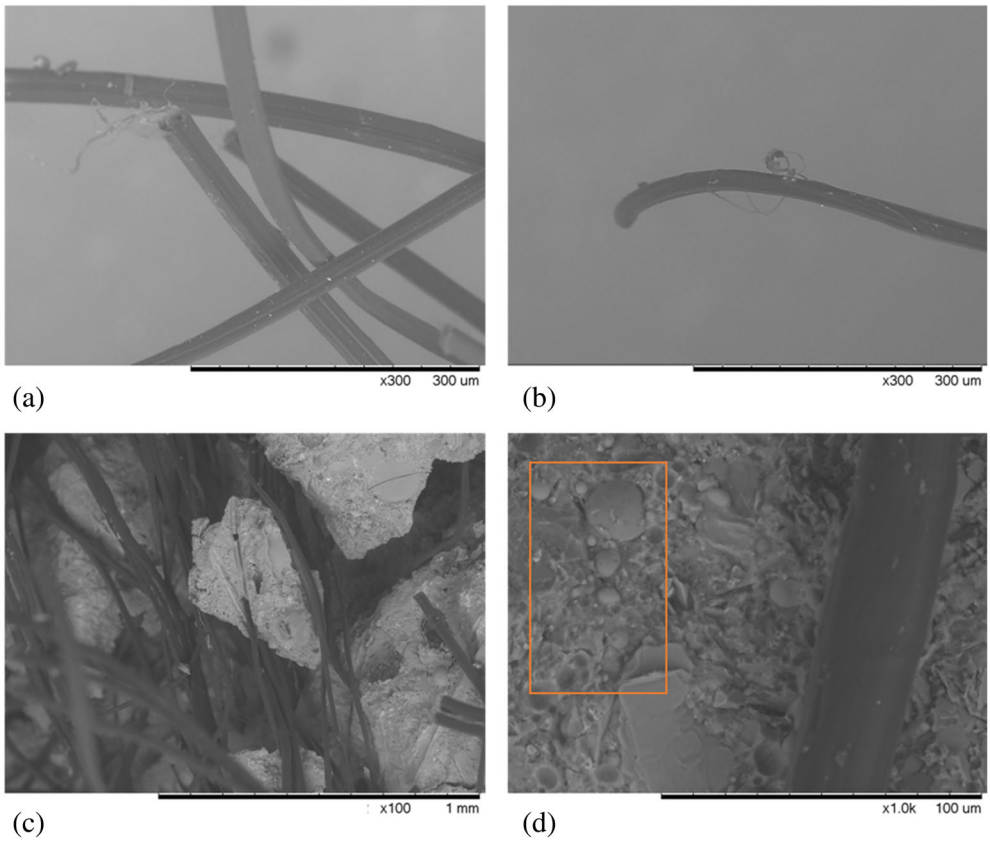

FIGURE 9 Scanning electron microscope observations on polyethylene fibers and matrix at 28 days.

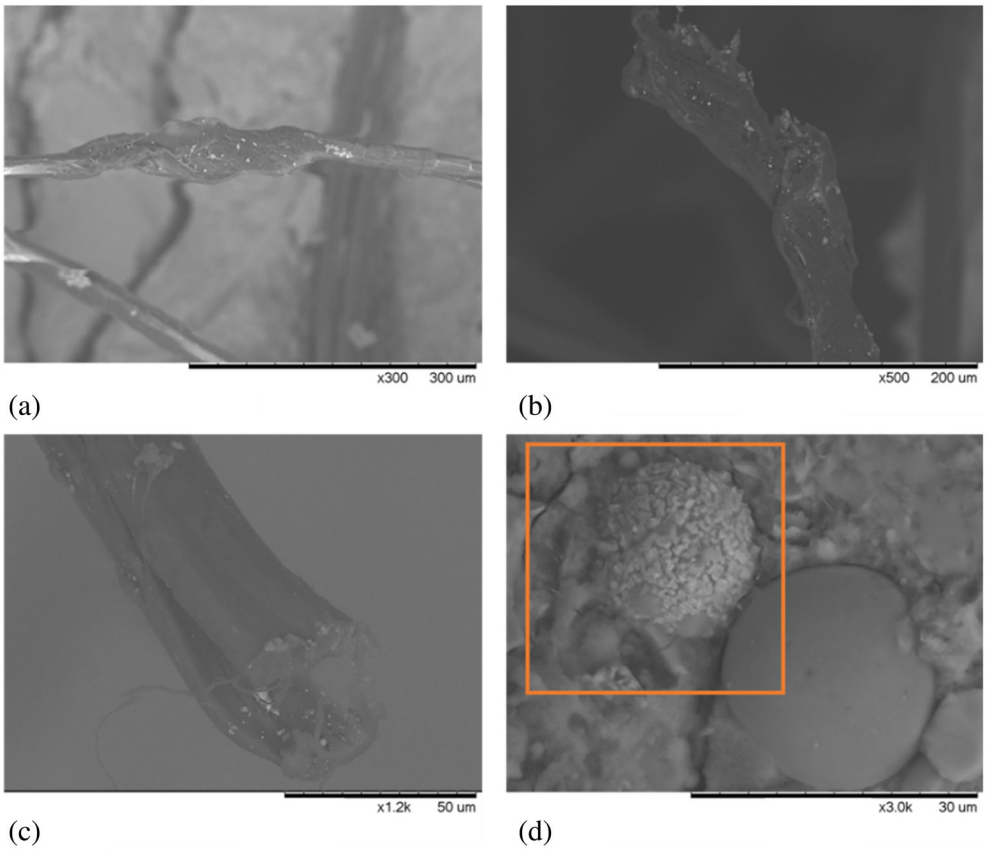

FIGURE 10 Scanning electron microscope observations on polyethylene fibers and matrix at 3 years.

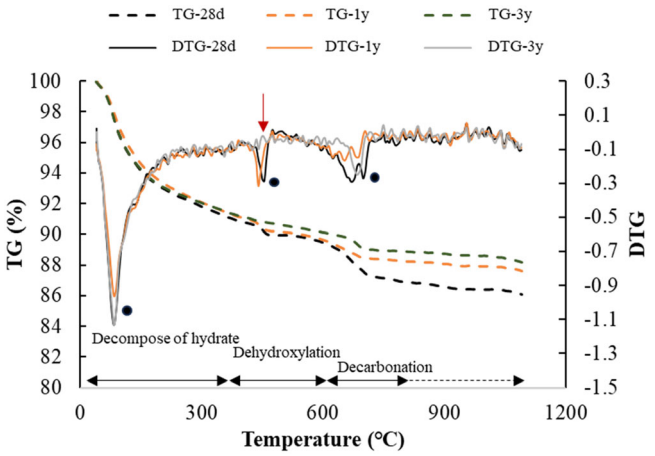

FIGURE 11 TG and derivation of the TG (DTG) curves of hybrid engineered cementitious composites at different ages. 28d, 28 days; 1y, 1 year; 3y, 3 years.

TABLE 3 Hybrid engineered cementitious composites mass loss (%) at different temperature ranges and different ages from thermogravimetric analysis.

Age	25–400°C	400–600°C	600–800°C
28 days	9.13	1.34	2.55
One year	8.85	1.44	1.39
Three years	8.78	1.03	1.24

and decomposable hydrates exist at an early age. The amount of such water was reduced at later ages due to further hydration. Comparing the mass loss between 400 and 600°C due to the dehydroxylation of portlandite, a higher value of 1.44% was observed from samples at 1y. The higher content of portlandite confirmed continuous hydration. It should be noted that an even lower mass loss of 1.03% was observed for 3y. In particular, the 400–600°C peak (red downward arrow in Figure 11) disappeared on the DTG curve for the 3y sample. This confirms that most portlandite had been transformed to other forms due to continuous hydration. The transformation was significant due to the high volume of fly ash and silica fume used in this mix design, which allows the portlandite to react with reactive silica, that is, SiO_2 for secondary hydration. These results agree with previous findings that nearly zero fly ash starts a pozzolanic reaction at 28d, and more than 80% of the fly ash remains unreacted even after 90 days of curing.[14,15] Although the detailed formations of hydration products and their transitions are not given here due to the limit of thermogravimetric analysis, peak changes in TG and DTG curves showed that hydration continued for up to 3 years. Such a long-term and slow hydration process thus may lead to gradual changes in the mechanical properties, which are discussed in the following sections.

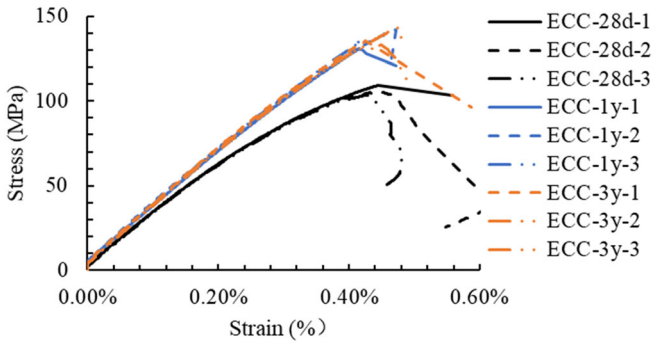

FIGURE 12 Compressive stress–strain curves of hybrid engineered cementitious composites at 28 days (28d), 1 year (1y), and 3 years (3y).

4.3 | Compressive properties and Young's modulus

Figure 12 shows the compressive stress–strain curves of hybrid ECC at different ages. It is observed that the compressive strength increased as age increased. Table 4 shows the compressive strength and the compressive strain at the peak load for samples with different curing ages. As shown in Table 4, the average compressive strength increased by 28% from 106.0 MPa at 28d to 136.2 MPa at 1y. Table 4 also shows that the average compressive strength was only slightly increased to 137.4 MPa at 3y. These results demonstrate that the change in compressive properties mainly occurs during the first year of curing. The increase in compressive strength was due to the gradual development of the hydration process. For the compressive strain at the peak load, Table 4 shows that there was virtually no change after 28d of curing.

Table 5 lists the Young's modulus of the hybrid ECC at different ages. It shows that the Young's modulus increased from 30.5 GPa at 28d to 34.1 GPa at 1y and then to 34.3 GPa at 3y. The increasing trend of Young's modulus agrees with the trend of compressive strength development, so that a significant change was only observed at 1y.

Hence, in terms of *compressive properties* of the hybrid ECC studied, an overall *improvement* after 1 year of curing was observed as there is a significant increase in both the compressive strength and Young's modulus, while the compressive ductility was unchanged.

TABLE 4 Summary of compressive properties of hybrid engineered cementitious composites (ECC) at different ages.

Specimen	Strength (MPa)	Average (MPa)	Compressive strain (%)	Average (%)
ECC-28d-1	109.3	106.0	0.46	0.45
ECC-28d-2	105.2		0.45	
ECC-28d-3	103.6		0.43	
ECC-1y-1	131.0	136.2	0.48	0.45
ECC-1y-2	141.9		0.46	
ECC-1y-3	135.6		0.42	
ECC-3y-1	135.8	137.4	0.42	0.45
ECC-3y-2	143.3		0.48	
ECC-3y-3	133.2		0.45	

Note: 28d, 1y, and 3y are specimens cured for 28 days, 1 year, and 3 years, respectively.

TABLE 5 Young's modulus of hybrid engineered cementitious composites (ECC) at different ages.

Specimen	Modulus (GPa)	Average (GPa)
ECC-28d-1	30.6	30.5
ECC-28d-2	30.5	
ECC-28d-3	30.5	
ECC-1y-1	33.9	34.1
ECC-1y-2	33.7	
ECC-1y-3	34.8	
ECC-3y-1	33.4	34.3
ECC-3y-2	34.3	
ECC-3y-3	35.3	

Abbreviations: 28d, 28 days; 1y, 1 year; 3y, 3 years.

4.4 | Tensile properties and cracking behavior

Figure 13 shows the stress–strain relationship and cracking behavior of hybrid ECCs at 28d, 1y, and 3y. Table 6 summarizes the tensile properties at different ages. Figure 13 and Table 6 confirm that the tensile strength of the hybrid ECC increased with age. As shown in Table 6, the average tensile strength increased by 7.5% from 5.87 to 6.31 MPa from 28d to 1y. Furthermore, the tensile strength also showed a small increase to 6.72 MPa at 3y. It should be noted that no potential degradation of PE fiber over time is considered in this work. As a previous study confirmed that polymer fibers used, such as PVA, showed no potential degradation after 26 weeks of accelerated aging tests, which is equivalent to 70 years of natural weathering.[5] Since the PE fiber used in this study has even more stable chemical and physical properties than PVA fiber due to its ultra-high molecular weight,[24,25] no degradation is assumed. Considering the ultimate tensile strength of ECC is attributed to the fiber–matrix bridging effect after matrix cracking, such a continuous increase in tensile strength confirms the increasing bond strength between fiber and matrix due to the development of the hydration process.

However, Table 6 shows that the ultimate tensile strain *decreased* significantly at 1y and 3y when compared with the 28d strain. The average ultimate tensile strain at 1y and 3y was 1.02% and 1.00%, respectively. These corresponded to a drop of 53.4% and 54.3% when compared with the 28d strain, respectively. Such a decrease in tensile ductility resulted from the change in bond strength between PE fiber and matrix as the matrix strength increased continuously as hydration developed with age. At 28d, the fiber strength is generally higher than the average bond strength; therefore, more fibers are pulled out from the matrix (Section 3.1, Figures 4a and 5). This results in a higher ductility and ultimate tensile strain. However, as age increases, the average bond strength between the fiber and matrix increases. The fiber strength then becomes lower than the average bond strength. Therefore, more fibers are fractured and ruptured rather than pulled out from the matrix (Figures 4c and 6), and the ultimate tensile strain is reduced. Furthermore, when comparing the 1y and 3y samples, only a very small further reduction of 0.02% of the average ultimate strain was recorded. This shows that the ultimate tensile strain reduction rate slowed down significantly after 1 year of curing.

As the ultimate tensile strain of the hybrid ECC showed a significant drop after 1 and 3 years, such a significant reduction of ductility could lead to inappropriate structural design if the tensile properties determined at 28d were adopted for design purposes. For example, in a typical bridge link slab design, it may require that the hybrid ECC have a minimum ultimate tensile strain of 1.2%.[16] Given that the hybrid ECC has a high ultimate

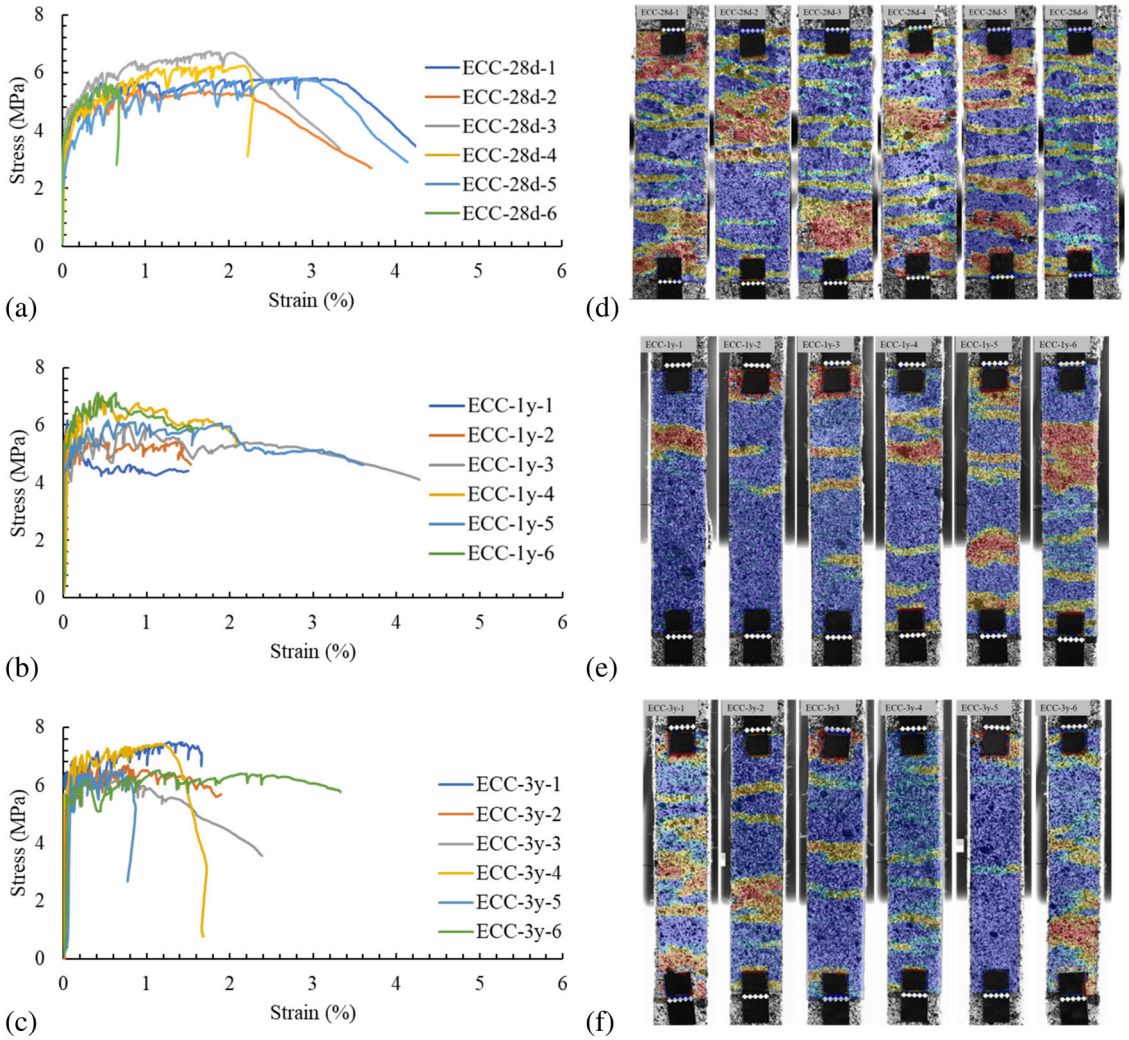

FIGURE 13 Tensile stress–strain curves of hybrid engineered cementitious composites (ECC) at (a) 28 days (28d), (b) 1 year (1y), and (c) 3 years (3y) and tensile cracking patterns at (d) 28d, (e) 1y, and (f) 3y.

tensile strain of 2.19% at 28d but only 1.02% after 1 year, if it were adopted for the construction, it may not be able to satisfy the design requirements in the long term.

Figure 13d–f and Table 6 also show the crack distributions and number of cracks through DIC analysis. As shown in Figure 13d, a saturated and intense cracking pattern was observed for 28d samples. On average, 15 cracks developed when the sample reached its ultimate tensile strain. However, the average number of cracks decreased to 8 and 7 for 1y and 3y samples, respectively. This shows that the hybrid ECC tended to develop larger local cracks (rather than micro-cracks distributed throughout the whole specimen) after 1 year of curing. Furthermore, when compared with 28d samples (Figure 13d), more and wider gaps between cracks were clearly observed on 1y (Figure 13e) and 3y (Figure 13f) samples. Thus, the cracking control ability of the hybrid ECC declined as its age increased. Such a decline in cracking control ability could definitely affect the long-term structural performance if the hybrid ECC was used in applications where the maximum crack size is a key performance parameter.

4.5 | Flexural properties

From the flexural test results, flexural strength was defined as the maximum tensile stress that occurred at the bottom surface of the beam in the pure bending region. Figure 14 shows the development of maximum tensile stress with the increase of deformation. The test results show good consistency among different samples tested. The flexural properties of the 28d and 3y samples tested are given in Table 7. It is observed that the

TABLE 6 Summary of tensile properties of hybrid engineered cementitious composites (ECC) at different ages.

Specimen		Tensile strength (MPa)	Average tensile strength (MPa)	Tensile strain (%)	Average tensile strain (%)	No. of cracks	Average no. of cracks
ECC-28d-1	5.73	5.87	3.03%	2.19%	15	15	
ECC-28d-2	5.31		2.21%		13		
ECC-28d-3	6.52		1.98%		15		
ECC-28d-4	6.22		2.12%		17		
ECC-28d-5	5.82		2.98%		13		
ECC-28d-6	5.61		0.82%		15		
ECC-1y-1	6.31	6.31	0.31%	1.02%	3	8	
ECC-1y-2	5.83		1.40%		5		
ECC-1y-3	5.84		0.99%		7		
ECC-1y-4	6.74		0.91%		8		
ECC-1y-5	6.06		1.89%		11		
ECC-1y-6	7.09		0.63%		13		
ECC-3y-1	7.15	6.72	1.45%	1.00%	11	7	
ECC-3y-2	6.68		0.73%		8		
ECC-3y-3	6.24		0.66%		7		
ECC-3y-4	7.19		1.29%		6		
ECC-3y-5	6.52		0.71%		3		
ECC-3y-6	6.52		1.14%		8		

Abbreviations: 28d, 28 days; 1y, 1 year; 3y, 3 years.

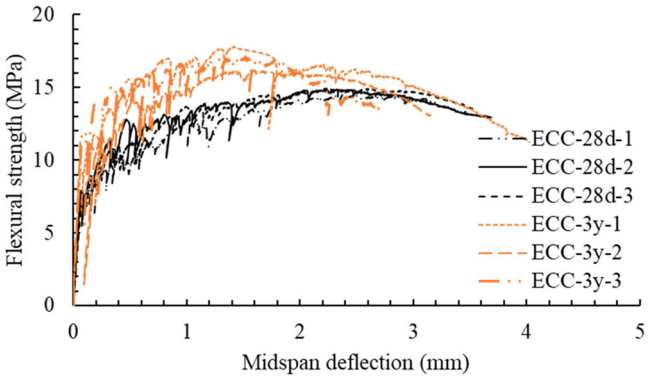

FIGURE 14 Flexural behavior of hybrid engineered cementitious composites (ECC) at 28 days (28d) and 3 years (3y).

average flexural strength of the hybrid ECC increased by 15% from 14.81 MPa at 28d to 17.04 MPa at 3y. This is expected as the modulus of flexural rupture is controlled by both the tensile strength and compressive strength, which were increased with age (Sections 4.3 and 4.4). Nevertheless, the deformation ability of hybrid ECC *decreased* as age increased. The maximum vertical deflection at the midspan of the specimen decreased by 35% from 2.35 mm at 28d to 1.51 mm at 3y, while the TCMOD decreased by 27% from 2.15 mm at 28d to 1.56 mm at 3y. Such a drop in flexural ductility agrees with the reduction of the tensile ductility (Section 4.4). As shown in Figure 15, all beams show a typical tensile bending failure mode. Cracks propagate from the bottom and develop along the height until failure. The decrease in deformation ability was caused by the decrease in ultimate tensile strain, as discussed in Section 4.4.

As shown in Figure 15a–c, 28d samples showed saturated and evenly distributed cracking patterns. The cracking pattern became more localized at 3y (Figure 15d–f) and cracks were concentrated near the two ends of the midspan region. This was because as further hydration developed with age, the PE fiber strength was lower than the average minimum cracking strength of the matrix; fibers were then prone to break and rupture before more cracks were developed. Without an effective fiber bridging effect, cracks became more localized. Such a reduction in cracking control ability is further confirmed in Table 7, which shows that the average number of cracks decreased from 25 (28d) to 13 (3y). Again, such a reduction in cracking control ability may not be desirable for some long-term structural applications where cracking control is a key performance requirement.

TABLE 7 Flexural properties of hybrid engineered cementitious composites (ECC) at different ages.

Specimen	Flexural strength (MPa)	Average flexural strength (MPa)	Vertical displacement	Average vertical displacement (mm)	TCMOD	Average TCMOD (mm)	Number of cracks	Average no. of cracks
ECC-28d-1	14.59	14.81	2.49	2.35	1.90	2.15	27	
ECC-28d-2	14.88		2.32		2.36		26	25
ECC-28d-3	14.95		2.24		2.19		23	
ECC-3y-1	17.80	17.04	1.41	1.51	1.70	1.56	15	
ECC-3y-2	16.21		1.59		2.19		18	14
ECC-3y-3	17.12		1.52		0.78		8	

Abbreviation: TCMOD, total crack mouth opening displacement; 28d, 28 days; 1y, 1 year; 3y, 3 years.

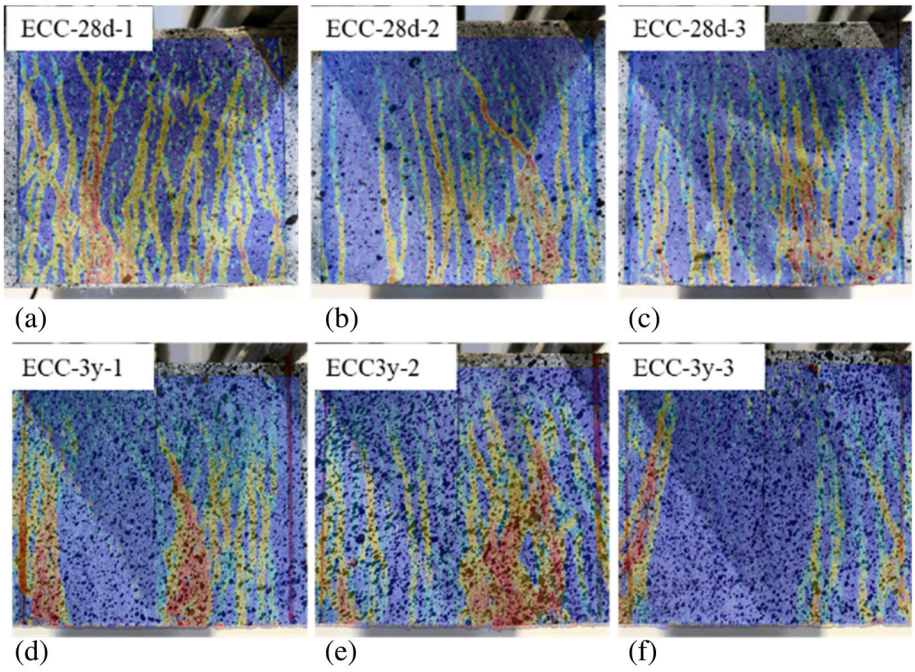

FIGURE 15 Bending cracking patterns of hybrid engineered cementitious composites (ECC) at 28 days (28d) (a–c) and 3 years (3y) (d–f).

5 | CONCLUSIONS

This work presents an experimental study of the long-term mechanical properties of a hybrid polyethylene-steel ECCs up to 3 years. The compressive, tensile, and flexural properties were obtained and compared at three different curing ages under standard curing conditions of 28d, 1y, and 3y. Microscopic observations and thermogravimetric analysis were conducted to understand the change in mechanical properties with increasing age. The conclusions drawn from the findings are listed below:

- From the microscopic observations and thermogravimetric analysis results, it is found that for the hybrid ECC studied, the hydration process had continued for 3 years with most of the hydration complete within 1 year. With the increase in age, continuous hydration led to an increasing fiber–matrix interaction and increased bond strength. This resulted in changes in failure mode from pull-out failure to rupture failure for PE fibers, but no change was observed for steel fibers due to their higher tensile strength.
- The experimental results show that the compressive strength of hybrid ECC increased as age increased. The average compressive strength increased by 28% from 106 MPa at 28d to 137 MPa at 3y, with most changes occurring within 1y. A similar increasing trend of Young's modulus was also observed. However, virtually no change was found for the compressive strain even after 3 years of curing.
- Similar to the compressive strength, both the tensile strength and the flexural strength of hybrid ECC increased as age increased. However, a significant reduction in the ultimate tensile strain and the flexural deformation ability was observed. In particular, the tensile strain and the flexural deformation ability were found to

have decreased by more than 54% and 35%, respectively, after 3y when compared with the 28d values. Such a reduction in ductility again largely occurred within 1y and was caused by continuous hydration. As a result, the average PE fiber–matrix bond strength was increased so that more PE fibers tended to rupture after a long curing period. Meanwhile, more serious localized cracks were observed for the 1y and 3y samples.

In summary, while increasing compressive, tensile, and flexural strengths of hybrid ECC are noted as age increases, a significant reduction in the tensile strain, flexural deformation ability, and cracking control ability was observed. The test results also confirmed that major changes in the mechanical properties of hybrid ECC could occur and become steady as early as after 1 year. These findings are invaluable for further development of the analytical model to predict long-term mechanical properties of hybrid ECC. These results also provide insights on hybrid ECC materials selection and safe structural design for applications such as bridge link slab and pavement constructions in which long-term ductility and cracking control ability are critical. Finally, it should be mentioned that different raw materials, fiber types, and fiber volume fractions in the mix design of hybrid ECC may have different impacts on their long-term mechanical properties, which shall be studied in future work.

ACKNOWLEDGMENT

Open access publishing facilitated by University of New South Wales, as part of the Wiley - University of New South Wales agreement via the Council of Australian University Librarians.

DATA AVAILABILITY STATEMENT

The data that support the findings of this study are available from the corresponding author upon reasonable request.

REFERENCES

1. Wang ZB, Zhang J, Wang JH, Shi ZJ. Tensile performance of polyvinyl alcohol–steel hybrid fiber reinforced cementitious composite with impact of water to binder ratio. J Compos Mater. 2014;49:2169–86. https://doi.org/10.1177/0021998314542450
2. Huang BT, Yu J, Wu JQ, Dai JG, Leung CK. Seawater sea-sand engineered cementitious composites (SS-ECC) for marine and coastal applications. Compos Commun. 2020;20:100353. https://doi.org/10.1016/j.coco.2020.04.019
3. Pakravan HR, Latifi M, Jamshidi M. Ductility improvement of cementitious composites reinforced with polyvinyl alcohol-polypropylene hybrid fibers. J Ind Text. 2014;45:637–51. https://doi.org/10.1177/1528083714534712
4. Lepech MD, Li VC. Long term durability performance of engineered cementitious composite. Restor Build Monum. 2006;12:119. https://doi.org/10.1515/rbm-2006-6038
5. Li VC, Horikoshi T, Ogawa A, Torigoe S, Saito T. Micromechanics-based durability study of polyvinyl alcohol-engineered cementitious composite. ACI Mater J. 2004;101:242–8. https://doi.org/10.14359/13120
6. Yu K, Lin M, Tian L, Ding Y. Long-term stable and sustainable high-strength engineered cementitious composite incorporating limestone powder. Structure. 2023;47:530–43. https://doi.org/10.1016/j.istruc.2022.10.008
7. Li VC, Wang S, Wu C. Tensile strain-hardening behavior or polyvinyl alcohol engineered cementitious composite (PVA-ECC). ACI Mater J. 2001;98:483–92.
8. Yu KQ, Wang YC, Yu JT, Xu SL. A strain-hardening cementitious composites with the tensile capacity up to 8%. Construct Build Mater. 2017;137:410–9. https://doi.org/10.1016/j.conbuildmat.2017.01.060
9. Lu C, Pang Z, Chu H, Leung CKY. Experimental and numerical investigation on the long-term performance of engineered cementitious composites (ECC) with high-volume fly ash and domestic polyvinyl alcohol (PVA) fibers. J Build Eng. 2023;70:106324. https://doi.org/10.1016/j.jobe.2023.106324
10. Kim M-J, Kim S, Yoo D-Y. Hybrid effect of twisted steel and polyethylene fibers on the tensile performance of ultra-high-performance cementitious composites. Polymers. 2018;10:879. https://doi.org/10.3390/polym10080879
11. Zhou H, Wu J, Wang X, Chen Y, Du X, Yu S. Performance of engineered cementitious composite (ECC) monolithic and composite slabs subjected to near-field blast. Eng Struct. 2023;279:115561. https://doi.org/10.1016/j.engstruct.2022.115561
12. Dong F, Yu K, Yu J, Wang Y, Liu K. Effects of environmental temperature on the mechanical properties of polyethylene fiber-engineered cementitious composites. Struct Concr. 2022;23:3114–25. https://doi.org/10.1002/suco.202100403
13. Fan Q, Zheng Y, He C, Meng D, Guo Q, Liu Y. Effect of interfacial properties between polyethylene and polyvinyl alcohol fiber/cement matrix on properties of mortar and ECC. Struct Concr. 2024. https://doi.org/10.1002/suco.202400607
14. Hanehara S, Tomosawa F, Kobayakawa M, Hwang KR. Effects of water/powder ratio, mixing ratio of fly ash, and curing temperature on pozzolanic reaction of fly ash in cement paste. Cem Concr Res. 2001;31:31–9. https://doi.org/10.1016/S0008-8846(00)00441-5
15. Lam L, Wong YL, Poon CS. Degree of hydration and gel/space ratio of high-volume fly ash/cement systems. Cem Concr Res. 2000;30:747–56. https://doi.org/10.1016/S0008-8846(00)00213-1
16. Zhu S, Zhang YX, Lee CK. Polyethylene-steel fibre engineered cementitious composites for bridge link slab application. Structure. 2021;32:1763–76. https://doi.org/10.1016/j.istruc.2021.03.104
17. C39M-18 AC. Standard test method for compressive strength of cylindrical concrete specimens. ASTM C39/C39M-18. 2018 https://doi.org/10.1520/c0039_c0039m-18
18. C469M-14 AC. Standard test method for static modulus of elasticity and Poisson's ratio of concrete in compression. ASTM C469/C469M-14. 2014 https://doi.org/10.1520/c0469_c0469m-14
19. Meng D, Huang T, Zhang YX, Lee CK. Mechanical behaviour of a polyvinyl alcohol fibre reinforced engineered cementitious composite (PVA-ECC) using local ingredients. Construct Build Mater. 2017;141:259–70. https://doi.org/10.1016/j.conbuildmat.2017.02.158
20. C1609M-12 AC. Standard test method for flexural performance of fiber-reinforced concrete (using beam with third-point loading). ASTM C1609/C1609M-12. 2012 https://doi.org/10.1520/c1609_c1609m-12

21. Jiang Y, Huo J, Qiao H, Lei Y, Jia L, Zhang Y. Synthesis of C-S-H accelerating admixture and its effect on mechanical and hydration properties of engineering cementious composites. Case Stud Constr Mater. 2024;20:e02993. https://doi.org/10.1016/J.CSCM.2024.E02993
22. Deboucha W, Leklou N, Khelidj A, Oudjit MN. Hydration development of mineral additives blended cement using thermogravimetric analysis (TGA): methodology of calculating the degree of hydration. Construct Build Mater. 2017;146:687–701. https://doi.org/10.1016/J.CONBUILDMAT.2017.04.132
23. Vogler N, Drabetzki P, Lindemann M, Kühne HC. Description of the concrete carbonation process with adjusted depth-resolved thermogravimetric analysis. J Therm Anal Calorim. 2022;147:6167–80. https://doi.org/10.1007/S10973-021-10966-1
24. Chhetri S, Bougherara H. A comprehensive review on surface modification of UHMWPE fiber and interfacial properties. Compos A Appl Sci Manuf. 2021;140:106146. https://doi.org/10.1016/J.COMPOSITESA.2020.106146
25. Forster AL, Forster AM, Chin JW, Peng JS, Lin CC, Petit S, et al. Long-term stability of UHMWPE fibers. Polym Degrad Stab. 2015;114:45–51. https://doi.org/10.1016/J.POLYMDEGRADSTAB.2015.01.028

AUTHOR BIOGRAPHIES

Shiyao Zhu, School of Engineering and Technology, University of New South Wales, Canberra, Australian Capital Territory 2600, Australia. Email: s.zhu@westernsydney.edu.au.

Y. X. Zhang, School of Engineering, Design and Built Environment, Western Sydney University, Kingswood, New South Wales 2751, Australia. Email: sarah.zhang@westernsydney.edu.au.

C. K. Lee, School of Engineering and Technology, University of New South Wales, Canberra, Australian Capital Territory 2600, Australia. Email: chi.k.lee@unsw.edu.au.

How to cite this article: Zhu S, Zhang YX, Lee CK. Long-term mechanical properties of hybrid fiber-reinforced engineered cementitious composite. Structural Concrete. 2025. https://doi.org/10.1002/suco.202400902